Journal of
Stem Cell Research & Therapy

Malecki et al., J Stem Cell Res Ther 2012, 2:5
DOI: 10.4172/2157-7633.1000130

Research Article Open Access

TRA-1-60+, SSEA-4+, Oct4A+, Nanog+ Clones of Pluripotent Stem Cells in the Embryonal Carcinomas of the Ovaries

Marek Malecki[a,b,*], Mark Anderson[a,c], Michael Beauchaine[d], Songwon Seo[a], Xenia Tombokan[e] and Raf Malecki[f]**

[a]*University of Wisconsin, Madison, WI, USA*
[b]*Phoenix Biomolecular Engineering Foundation, San Francisco, CA, USA*
[c]*National Institutes of Health, National Nuclear Magnetic Resonance Facility, Madison, WI, USA*
[d]*Bruker AXS, Fitchburg, WI, USA*
[e]*Bruker Optics, Dallas, TX, USA*
[f]*San Francisco State University, San Francisco, CA, USA*

Abstract

Introduction: Embryonal Carcinoma of the Ovary (ECO), pure or admixed to other tumors, is the deadly gynecological cancer.

Specific aim: The specific aim of this work was identification, isolation, clonal expansion, and molecular profiling of the pluripotent cells in the embryonal carcinomas of the ovaries.

Patients and methods: The samples were collected from the patients, who were clinically and histopathologically diagnosed with the advanced, pure ECO. Preparation of the samples was initiated by negative selection of the cells by MACS, while using the superparamagnetic scFvs against phosphatidylserine (PS), and dsDNA, CD45, CD34, CD19, CD14, and by positive selection, while using the superparamagnetic scFvs for TRA-1-60 and SSEA-4. The cell surface display was analyzed by flow cytometry (FCM), immunoblotting (IB), multiphoton fluorescence spectroscopy (MPFS), nuclear magnetic resonance spectroscopy (NMRS), and total reflection x-ray spectroscopy (TRXFS). The transcripts of the OCT4A and Nanog were analyzed by qRTPCR and MPFS. The human pluripotent, embryonic stem cells (ESC), human pluripotent, embryonal carcinoma of the testes (ECT), healthy tissues of the ovary (HTO), healthy tissue of the testes, peripheral blood mononuclear cells (PBMC), and bone marrow mononuclear cells (BMMC) served as the controls.

Results: The studied embryonal carcinomas of the ovary (ECO) contained the cells with significantly higher intensity of the surface display of the TRA-1-60 and SSEA-4, relative to the BMMC, PBMC, and HTO, but similar to the pluripotent ESC and ECT. Their morphology and ultrastructure were consistent with the histopathological diagnoses. Moreover, these cells were significantly stronger expressers of the Oct4A and Nanog, relative to the PBMC, BMMC, and HTO, but similar relative to the pluripotent ESC and ECT. The ECO cells formed embryoid bodies, which differentiated into ectoderm, mesoderm, and endoderm. These cells were induced to differentiate into muscles, epithelia, and neurons.

Conclusion: Herein, we revealed presence and identify molecular profiles of the clones of the pluripotent stem cells in the embryonal carcinomas of the ovaries. These results should help us with refining molecular diagnoses of these deadly neoplasms.

Keywords: Cancer of the ovary; Embryonal carcinoma of the ovary; Variable fragment antibody; Pluripotent stem cell; Tumor resistance antigen TRA-1-60; SSEA-4; Oct4A; Sox2; Nanog

Abbreviations: ECO: Embryonal Carcinoma of the Ovary; ECT: Embryonal Carcinoma of the Testis; TRA-1-60: Tumor Resistance Antigen 1-60; SSEA-4: Stage Specific Embryonic Antigen 4; OCT4A: Octamer-binding Transcription Factor 4A; Sox2: Sex Determining Region Y-box 2; Nanog: Homeobox Transcription Factor; scFv: Single Chain Variable Fragment Antibody; dcFv: Dual Chain Variable Fragment Antibody; f*scFv: Fluorescent scFv; s*scFv: Superparamagnetic scFv; FCM: Flow Cytometry; IB: Immunoblotting; MACS: Magnetically Activated Cell Sorting; FACS: Fluorescently Activated Cell Sorting; NMRS: Nuclear Magnetic Resonance Spectroscopy; TRXFS: Total Reflection X-ray Fluorescence Spectroscopy; MPFS: Multiphoton Fluorescence Spectroscopy; EELS: Electron Energy Loss Spectroscopy; EDXS: Energy Dispersive X-ray Spectroscopy.

Introduction

Cancer was the primary cause of deaths for women between the ages of 20-85 in the USA in 2010 [1]. Among them, more than 21,880 women were diagnosed with cancers of the ovaries (COs) and 13,850 of them died of that cause. The essential factor for the longest survival was the earliest diagnosis of cancer and prompt therapy. This was well exemplified by the statistics, which showed the 84.1% 10-year survival rate for women diagnosed at the FIGO's early clinical stage Ia, but down to the 10.4% 10-year survival rate for those diagnosed at the advanced stage III [2,3]. Unfortunately, 63% of women were diagnosed after the cancers have already progressed to the advanced stages. These findings have branded ovarian cancer "silent killer", as the most deadly among all gynecological neoplasms [1,2].

At the early stages of this disease, women may not feel any symptoms.

***Corresponding author:** Marek Malecki, MD, PhD, UW, Madison, WI and PBMEF, San Francisco, CA, USA, Tel: 4157134370; E-Mail: mm@pbmef.org

Received October 08, 2012; **Accepted** November 15, 2012; **Published** November 18, 2012

Citation: Malecki M, Anderson M, Beauchaine M, Seo S, Tombokan X, et al. (2012) TRA-1-60+, SSEA-4+, Oct4A+, Nanog+ Clones of Pluripotent Stem Cells in Embryonal Carcinomas of the Ovaries. J Stem Cell Research and Therapy 2: 130. doi:10.4172/2157-7633.1000130

Later, the symptoms may include transient abdominal discomforts, bloating, pains, urinary urgencies, as well as other symptoms non-specific for genital system [4-6]. These symptoms prompt them to visit physicians followed by referrals to clinical laboratories.

The lab test of choice is measurement of CA125 in sera of the patients; however, its poor sensitivity prompts efforts to seek other biomarkers by analysis of proteins, microRNA, and circulating tumor cells (CTCs) [7-18]. Initial screenings with ultrasonography (USG) are very promising; however, its relatively poor resolution leads to follow-up imaging with high resolution CT or MRI, which do not yet define the cancers' lineage [19-21]. Cancer progression is defined through clinical staging according to FIGO, whereas after initial progression in situ, which is denoted as the stage I, the cancers grow as pelvic masses. From the moment of the cells' break out into the peritoneal cavity, they become detected in ascites, which is specifically denoted as the stage Ic. Thereafter, the cancer cells invade the pelvic organs - stage II and subsequently metastasize to distant organs denoted as the stages III and IV [3]. The final diagnosis is based upon histopathology, which identifies the tumor cells' lineage. Almost 90% of the ovarian neoplasms have epithelial origins. Although rare, the germ cell tumors (GCTs) are very malignant. Among them, pure or admixed embryonal carcinomas of the ovary (ECO) are most deadly malignant tumors [2,3,22,23]. Moreover, they are most difficult to diagnose including lab tests, since they do not secrete AFP and hCG as the other GCTs. The ECO cells retain morphological features of pluripotent, undifferentiated, embryonic cells in the pure ECOs and in admixes to other compound tumors. However, they frequently differentiate into teratomas, which resemble various somatic cell lineages. These characteristics make patomorphology based diagnoses difficult. They make diagnoses even harder in cases of anaplastic tumors. Therefore, molecular profiling of these cells should help not only with distinction between the epithelial and germ cell tumors, but also with search for clones of therapy resistant stem cells, as essential steps towards targeted, personalized therapies [24-30].

Several biomarkers were identified as biomarkers of multipotent cells in epithelial ovarian cancers (EOC), including standard version and variants of the CD44, CD133, MyD88, EpCAM [31-42]. However, none of them identified pure populations of the pluripotent stem cells, nor defined molecular profiles of the germ cell tumors of the ovaries. Moreover, in our hands, sorting for those markers resulted in heterogeneous populations of the cells; thus with variety of molecular profiles and biological properties. The neoplasms, which could be identified as the closest to the embryonal carcinomas of the ovaries were the embryonal carcinomas of the testes [22,23,43-58]. Testicular, extragonadal, and ovarian embryonal carcinomas, all share the same morphology. Molecular profiles of the human, pure embryonal carcinoma cells of the testes revealed their pluripotency equal to that of the human embryonic stem cells (hESC) [43,50]. This included their ability for self-renewal and differentiation into the three germ lineages. Molecular profiles of the ECO cells have not been defined.

In this regard, our interest was focused on TRA-1-60 and SSEA-4 [43-58]. They were defined as the stem cells' hallmarks of pluripotency. They were shown to be the unique biomarkers of the pluripotent testicular embryonal carcinoma cells, which ceased to express upon their differentiation. Moreover, TRA-1-60 was identified on cells in sections from the ECT biopsies [57]. It was also detected being shed into blood of the patients with the ECT [14,58]. However, it was not displayed on the healthy, differentiated cells. Similarly, SSEA-4 was uniquely expressed on the undifferentiated, pluripotent ESCs' and ECTs' cells only, but completely absent from the cells upon their differentiation [45,48]. These biomarkers were never tested on the ECOs. Furthermore, of our great interest was also the triad of the transcription factors being indicators of the cells' pluripotency: Oct4, Sox2, and Nanog [59-62]. In particular, from at least three alternative splicing transcripts (OCT4A, OCT4B, OCT4B1) and four alternative translation isoforms (OCT4A, OCT4B-190, OCT4B-265, and OCT B-164), only OCT4A was shown to be the master switch of pluripotency. While strong expression of the OCT4 was measured in the ESCs and ECTs, it was not detected in the healthy tissues [55]. The pure populations of the embryonal carcinomas of the ovary (ECO) have not yet been studied and characterized in this regard.

Accordingly, the specific aim of this work was identification, isolation, clonal expansion, and molecular profiling of the pluripotent cells in the embryonal carcinomas of the ovaries using aforementioned biomarkers.

Materials and Methods

Patients and samples

All the samples were obtained in accordance with the Declaration of Helsinki, with the Institutional Review Boards' approval, and with the Patients' Informed Consent. The samples from patients, who were being clinically and histopathologically diagnosed with the germ cell tumors (GCT): women with ovarian GCTs (n=43); men with testicular GCTs (n=103); women (n=3) or men (n=3) with the extragonadal GCTs were included into this study. All the samples were encoded to protect the patients' identity. The six cases of the pure embryonal carcinomas of the ovaries (ECO) were selected for this study. Collection of the samples from the pelvic mass, ascites, metastases, healthy tissue margins, bone marrow, and blood was performed according to the standard surgical procedures. The batches of the samples were either immediately labeled with the single or dual chain variable fragment (Fv) antibodies, or incubated for cultures / clonal expansion, or rapidly cryoimmobilized or chemically preserved as described [63-70].

Genetically engineered single or dual chain variable fragment (Fv) antibodies

The single or dual chain variable fragment antibodies (scFvs) were prepared as described previously [29,48,69,70], thus only briefly outlined below. The pooled B cells from the patients suffering from cancers were used to isolate mRNA, reverse transcribe, and create the cDNA libraries of complementarity determining regions (CDR) and framework regions (FWR) for anti-cancer-antibodies (ACA) coding sequences. The cds, after insertion into the plasmids containing chelates harboring coding sequences under the CMV promoters, were propagated and expressed in human myelomas as described (clones scFv TRA-1-60 24, SSEA-4 37 were used in this project). The TRA-1-60 and SSEA-4 were purified, which followed by modification with biotin or digoxigenin. The modified TRA-1-60 or SSEA-4 were anchored onto anti-biotin or anti-dig saturated pans and served as baits for selection of the Fv clones from the ACA libraries. The chelates were saturated with Gd, Tb, Eu. The elemental compositions were quantified with the scanner S2 Picofox (Bruker AXS, Fitchburg, WI). The fluorescent properties were measured with the RF-5301PC spectrofluorometer (Shimadzu, Tokyo, Japan). The relaxivities were measured on the DMX 400 WB or AVANCE II NMR spectrometers (Bruker Optics, Dallas, TX). The specificity and sensitivity of the scFvs were tested with the EELS and EDXS [67]. The monoclonal antibodies targeting TRA-1-60

and SSEA-4 served as the controls as characterized [45].

Cultures and clonal expansion of embryonal carcinoma cells of the ovaries

The cancer cells were grown in semi-fluid cultures as described and thus only briefly outlined here [43,44,63]. Cell clusters were separated into single cell suspension by short treatment with the PIPES buffered DNase, RNase, hyaluronidase, trypsin, and collagenase. The cells were isolated by MACS as described [29]. The substrates for cultures consisted of two layers of 1.2% and 0.6% Matrigel in DMEM medium supplemented with 20% human serum, 2 mM L-glutamine, 100 U/mL of Penicilin, 100ug/mL of Streptomycin, 1% nonessential amino acids. The cultures were maintained in the incubator at 37°C with controlled 0.1% O_2, 5% CO_2, 94.9% N_2 and saturated humidity environment. The cultures of the human embryonic stem cells - hESC H1, H7, H9 and human metastatic embryonal carcinoma of the testis cells - hECT NT2D1, muscle cells - RD, brain neuronal cells - HCN-2 cultures were the controls as originally described (ATCC, Manassas, VA) [45]. Embryoid bodies were cultured as described originally for the testicular carcinomas [43,44]. Moreover, the healthy ovarian tissue (HTO) from prophylactic oopherectomy or margins surrounding the tumor, healthy tissue of testes (HTT) dissected during orchiectomy, healthy margins of the brain removed during the brain surgery, and healthy margins of cardiac tissue excised during cardiac surgery were the controls. For testing differentiation of the embryoid bodies into the three germ layers, they were labeled with the antibodies for myosin – as the marker of the mesoderm formation, keratin – as the marker of the endoderm formation, and 68kDa neurofilaments protein- as the marker of the ectoderm formation. For inducing differentiation, the cells were exposed to 10^{-5} M retinoic acid, 1 % DMSO, 3 mM hexamethylene bisacetamide (HMBA), 1% dimethylsulphoxide (DMSO), 250 ng/ml nerve growth factor, epidermal growth factor, or vascular endothelial growth factor as described (Sigma-Aldrich, Saint Louis, MO, USA) [51,52]. The evaluation of differentiation was based upon labeling with the Fv antibodies anti-myosin - to validate differentiation into muscle, anti-NF68 neurofilaments – to validate differentiation towards neurons, and anti-CK18 cytokeratins – to validate differentiation towards epithelia [48].

Cryo-immobilization

The cells were injected into the sterile, gold planchettes, loaded, and cooled down to –196°C within 10 ms at 2000 atm within the high pressure freezing machine HPM10 (Bal-Tec, Balzers, Liechteinstein) [67]. Alternatively, they were frozen with the melting ethane-based cryo-immobilization machine (the cryo-station built with the NSF funds – PI: Dr M. Malecki). The frozen samples were promptly transferred to and stored in liquid nitrogen dewars. For cultures, the samples were thawed directly into the culture media. For ultrastructural studies, they were prepared by freeze-substitution in the FSD010 (Bal-Tec, Balzers, Liechteinstein), low temperature embedding, and cryo-sectioning or freeze-fractured and freeze-dried on the BAF400 (Bal-Tec, Balzers, Liechteinstein). Evaluation of the freezing procedure was pursued on the cryo-sections cut on the cryo-ultratome (Leica, Buffalo Grove, IL) and transferred within the cryo-transfer system on the energy filtering system 912 Omega (Zeiss, Oberkochen, Germany) to assure absence of ice segregation determined upon diffraction patterns.

Chemical fixation

For the ultrastructural overview, the cells were fixed by adding up to 4% formaldehyde, 0.1% glutaraldehyde, 0.2 % tannic acid (Pella, Redding, CA) [44]. Thereafter, they were either frozen, freeze-substituted, embedded in epon 812 (Ladd, Williston, VT), and sectioned on the ultratome (Leica, Buffalo Grove, IL) or rinsed in the physiological buffer attached to the silane coated gold or carbon carriers, dried in the critical point of CO_2, and cryo-sputter coated with a monomolecular layer of Cr or Pt/C on the BAF400 (Bal-Tec, Balzers, Liechteinstein).

Immunoblotting (IB)

The cells were either frozen in liquid nitrogen, crushed, and thawed or/and disintegrated with ultrasonicator (Branson Ultrasonic, Danbury, CT) within the sample buffers for native protein analysis. They were stored in liquid nitrogen or electrophoresed in the native buffer (Invitrogen, Carlsbad, CA). They were vacuum or electro-transferred onto the PVDF membranes (Amersham, Buckinghamshire, UK). The membranes carrying transferred proteins were soaked within human serum and labeled with the Fvs. The samples of muscle myosin, neuronal NF68, and keratin served as the controls. The images of the blots were acquired and quantified with Fluoroimager (Molecular Dynamics, Sunnyvale, CA) or Storm 840 (Amersham, Buckinghamshire, UK). The levels of the products were also calculated as the ratio between the protein concentration in the examined patient's cells and the controls.

Quantitative reverse transcription and polymerase chain reaction (qRTPCR)

Nucleic acids were isolated using the Nucleic Acid Extractor Model 340A (ABI). The total isolated mRNA served as the template to generate cDNA through reverse transcription using random hexamers and reverse transcriptase (ABI, Foster City, CA, USA) as described [29]. The cDNAs and amplicons quality was tested by polymerase chain reaction of beta actin and GAPDH as the reference genes (ABI, Foster City, CA, USA). For evaluation of the gene expression levels for Oct4A, OCT4B, OCT4B, the primers sets were designed using Primer Express (ABI, Foster City, CA, USA) based upon the sequences imported from the Public Domain GenBank (NCBI), and synthesized on the 380A DNA Synthesizer (ABI, Foster City, CA, USA). The PCR and qPCR reactions were carried using the mix of the cDNA, the synthesized primers, dNTPs, and Taq DNA polymerase (Hoffmann–La Roche, Basel, Switzerland) on the Robocycler (Stratagene, San Diego, CA), Mastercycler (Eppendorf, Hamburg, Germany), or 7500, 7900 HT qPCR systems (ABI, Foster City, CA, USA). The images of the gels were acquired and quantified with Fluoroimager (Molecular Dynamics, Sunnyvale, CA) or Storm 840 (Amersham, Buckinghamshire, UK). The levels of the transcripts were first normalized against GAPDH or actin and thereafter calculated as the ratio between the transcript concentration in the examined patient's cells versus the cells from the HTO, HTT, BMMCs, PBMC, hESCs, or hECT cells.

Flow cytometry (FCM), fluorescently activated cell sorting (FACS) and multiphoton fluorescence spectroscopy (MPFS).

The cell clusters were thoroughly disintegrated. The negative selection involved depletion of white blood cells with the superparamagnetic Fvs (s*Fvs) antiCD45, CD34, CD19, CD14; the apoptotic cells were removed with the s*Fvs against phosphatidylserine, the dead cells were eliminated with the s*Fvs against dsDNA [70]. The remaining samples were further enriched by the positive selection with the s*scFv for TRA-1-60 or SSEA-4. The side population was determined with the Hoechst 33342 in Verapamil tests (Sigma-Aldrich, Saint Louis, MO, USA). The enriched populations of cells labeled with the fluorescent scFv targeting

TRA-1-60 or SSEA-4 were measured with the Calibur, Vantage SE, or Aria (Becton-Dickinson, Franklin Lakes, NJ) or the FC500 (Beckman-Coulter, Brea, CA). The fluorescently labeled cells were imaged with the Axiovert (Zeiss, Oberkochen, Germany) equipped with the Enterprise argon ion (457 nm, 488 nm, 529 nm lines) and ultraviolet (UV) (364 nm line) lasers; Odyssey XL digital video-rate confocal laser scanning imaging system operated up to 240 frames/s under control of Intervision software (Noran, Madison, WI), and the Diaphot (Nikon, Tokyo, Japan) equipped with the Microlase diode-pumped Nd:YLF solid state laser (1048 nm line), the pulse compressor with the pulses' rate 300 fs at 120 MHz and the MRC600 scanning system under control of Comos software (the multi-photon station built with the NIH funds – PI: Dr J. White). Images were deconvolved after their import to the Indy workstation (Silicon Graphics, Fremont, CA).

Total reflection x-ray fluorescence spectroscopy (TRXFS)

In this study, the ICP standard of 1000 mg/l of mono-element Gallium (CPI International, Denver, CO) was added to 500 microL of each sample for a final concentration of 10 mg/l. The data were generated from a S2 Picofox TXRF spectrometer equipped with a molybdenum (Mo) X-ray target and the Peltier cooled Xflash Silicon Drift Detector (Bruker AXS, Fitchburg, WI). Scan times ranged up to 1000 seconds. The automatic sample changer which can hold up to 25 samples was also used along with the SPECTRA 7 software for instrument control, data collection, and analysis (Bruker AXS, Fitchburg, WI).

Nuclear magnetic resonance (NMR) and magnetically activated cell sorting (MACS)

The cells were labeled for positive selection with the superparamagnetic Fvs (s*Fv) targeting TRA-1-60, and for the negative selection targeting CD45, CD34, CD14, CD19, dsDNA, and PS, while suspended in the physiological buffer supplemented with serum and glucose [68]. The small aliquots were dispensed into the magnetism-free NMR tubes (Shigemi, Tokyo, Japan). The relaxation times T1 were measured in resonance to the applied FLAIR pulse sequences on the NMR spectrometers DMX 400 WB or AVANCE II NMR (Bruker, Billerica, MA) or the Signa clinical scanners (GE, Milwaukee, WI). The s*Fvs were also used to isolate the labeled cells from the solution using the 1.5 T magnetic sorter (the sorter designed and built based upon the NSF funds – PI: Dr M. Malecki) [29].

Electron energy loss spectroscopy (EELS) and energy dispersive x-ray spectroscopy (EDXS)

The samples, which were cryo-immobilized, presented the life-like supramolecular organization. Molecular imaging was pursued as described [67]. The energy filtering transmission electron microscopes Zeiss EM912 and 922 with the LaB6 sources were equipped with the Omega electron energy loss spectroscope (EELS). The microscopes were equipped with the Oxford's and Fishione's cryo-transfer systems. Images were acquired on the Gatan lkxlk CCD camera and processed with the SIS software. The Philips' CM420 with LaB6 source was equipped with the Gatan post-column electron energy loss (EELS) and Noran's energy dispersive x-ray (EDXS) spectrometers. The microscope was also equipped with the Gatan's cryotransfer system. Images were acquired and processed with the Gatan's MS software. The Zeiss SEM1540, Hitachi H3400, and JEOL's JSM 6000 field emission scanning electron microscopes were equipped with their own EDXS spectrometers. Structural and elemental analysis was pursued in three steps. First, the complete elemental spectra were acquired for every pixel of the scans to create the elemental databases. Second, the elemental distribution maps were extracted from those databases. Third, elemental distributions were merged with other elemental maps or superimposed over the architectural data. This approach allowed us to identify molecular architecture of the analyzed cells and organelles.

Statistical analysis

Fisher's exact test was used to examine the association of the gene expression between the human ECO cells versus the controls: cultured human embryonal carcinoma cells of the testis (NT2D1), embryonic stem cells (H1, H7, H14), healthy tissue of the ovaries (HTO), or peripheral blood mononuclear cells (PBMC), or bone marrow mononuclear cells (BMMC). Average gene expression measurements were run in triplicates for each patient and control, which were used for gene expression statistical analysis. For the comparisons, Wilcoxon signed rank test was used, and Wilcoxon rank sum test for the comparison of two independent groups of the ECO versus the ECT and ESC cells. A two-sided p-value was computed in each comparison. The graphs were displayed using GraphPad software (GraphPad Software, Inc, La Jolla, CA).

Results

The cell populations from biopsies were enriched by negative selection in MACS with the superparamagnetic Fv targeting CD45, CD34, CD14, CD19, CD20 to deplete the samples of the white blood cells (WBC), with the Fvs against dsDNA and phosphatidylserine to deplete from the dead and apoptotic cells. They were further enriched by positive selection with the superparamagnetic Fv targeting TRA-1-60 and SSEA-4. The evaluation of the surface displayed molecules on the ECO versus the ESC and ECT cells was performed on the cells labeled with the fluorescent Fv against TRA-1-60 and imaged with multiphoton fluorescence microscopy as shown in the figure 1. The labeling of the cells is very intense and specific. The background is clean. The positive controls, the cells of cultures of the hESC H7 and hECT NT2/D1, were identified by the same labeling protocol. This morphological evaluation was followed by the statistical analysis of the labeling kinetics presented in the figure 2. The TRA-1-60 display on the ECO cells was only slightly statistically higher than on the ESC and ECT cells. The TRA-1-60 display was not detected on the PBMCs and BMMCs.

Indentation homogenous populations of cells are really necessary to determine their molecular profiles. For that reason, the populations

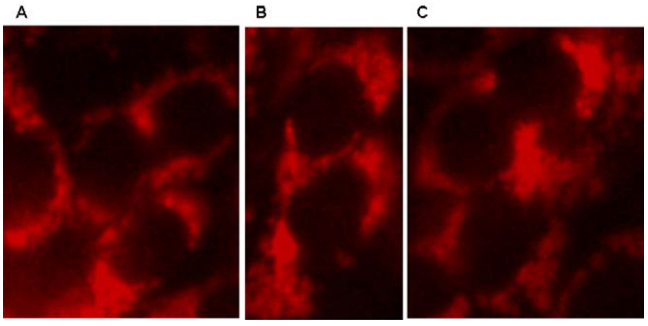

Figure 1: Display of TRA-1-60 on the ECO cells. The ECO, ESC, and ECT cells were labeled with the fluorescent scFv targeting TRA-1-60. They were imaged with multiphoton fluorescence. The kinetics of labeling was determined upon the digital quantum intensity profiles presented in the figure 3. Intensity and pattern of labeling of the ECO cells (A) is identical to the ESC (B) and ECT (C) cells. Magnification: 1,000 x.

were enriched by sorting and their purities were evaluated by flow cytometry as shown in the figure 3. It revealed that the enrichment resulted in more than 99% purity of the sorted cell populations. The statistical analysis of enrichment was presented in the figure 4. Sorted populations of the ECO cells appeared to have identical profiles to those of the hESC and hECT cells used as the positive controls. The populations of the PBMC and BMMC cells, which served as the negative controls showed no specific labeling similar to the isotype antibody profiles. Purity of the enriched populations of the cells and labeling intensity values were contingent upon the specificity of labeling for TRA-1-60, which was measured at the full width at half-maximum (FWHM) for each run, averaged, and calculated for statistical significance. The statistical significance was approved at the $p < 0.001$.

For the further analysis of the cell surface displayed molecular profiles, the cells were rapidly cryoimmobilized. This followed by homogenization, electrophoresis, and transfers onto the PVDF membranes. The molecules on membranes were labeled with the Fv targeting TRA-1-60 and imaged as illustrated in the figure 5. The labeling is very strong and specific. There is no other labeling along the lanes except the single, strong, specific bands. The labeling is identical to that seen for the molecules gained from the ESC and ECT cells used as the positive controls. The PBMC and BMMC cells, serving as the negative controls did not absorb any labeling. The statistical analysis

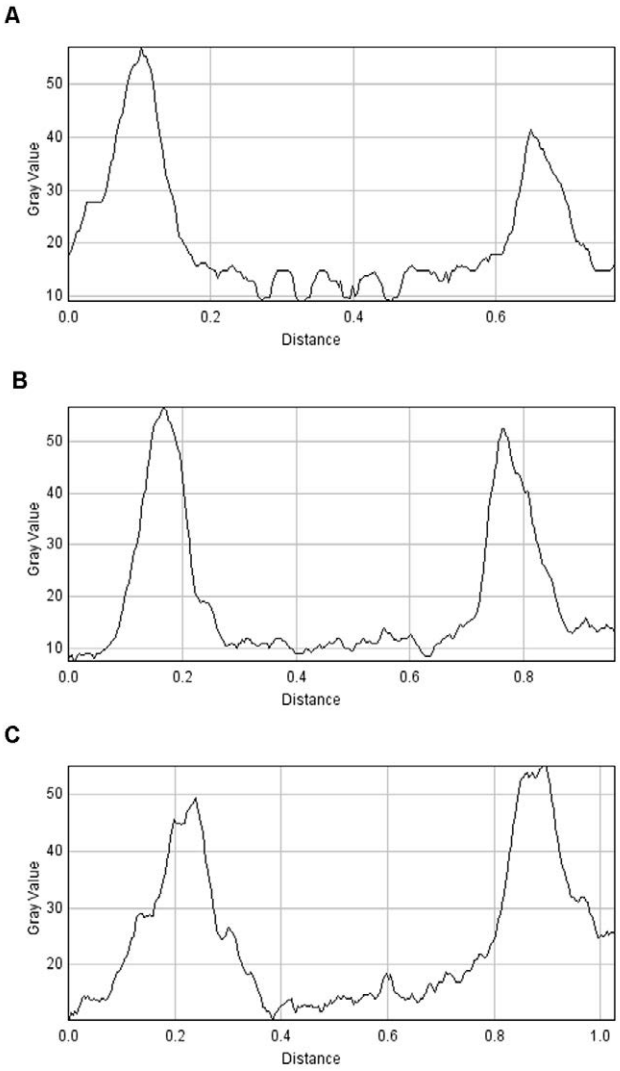

Figure 2: Quantified kinetics of the TRA-1-60 display on the ECO cells. The images of the ECO, ESC, ECT cells acquired as described in the figure 2 were quantified by measuring pixel intensity values across the cells' diameters to reveal the kinetics of the scFv display. They show identical kinetics of labeled the ECO (A), ESC (B), and ECT (C) cells. They also demonstrate the identical, high ratio between the nucleoplasm and cytoplasm is all these cells.

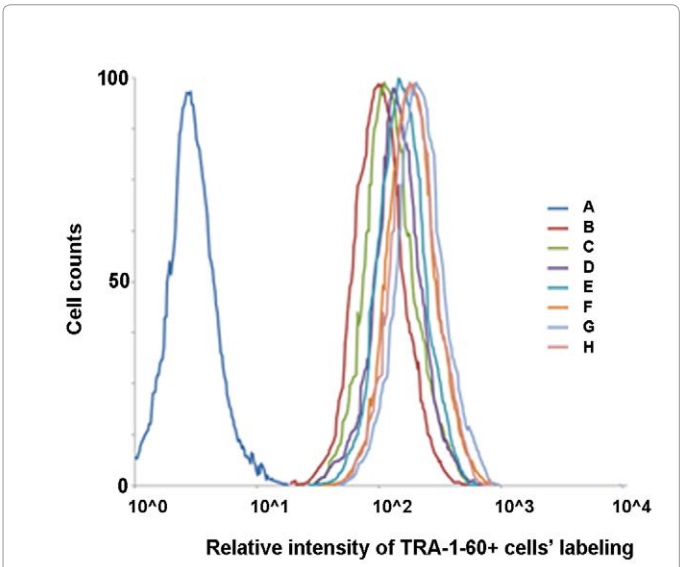

Figure 3: TRA-1-60+ enriched populations of the ECO cells. The ECO cells were labeled with the fluorescent scFv targeting TRA-1-60 after population enrichment selection by MACS. Labeling: the patients' ovarian embryonal carcinoma cells (A-F), the embryonic stem cells (G) and the bone marrow mononuclear cells (H). Statistical significance was accepted for the $p < 0.001$ with the values of the FWHM between the patients' readings and the negative controls, while there was no significant statistical difference in the intensity between the patients' cells and the positive controls as quantified in the figure 4.

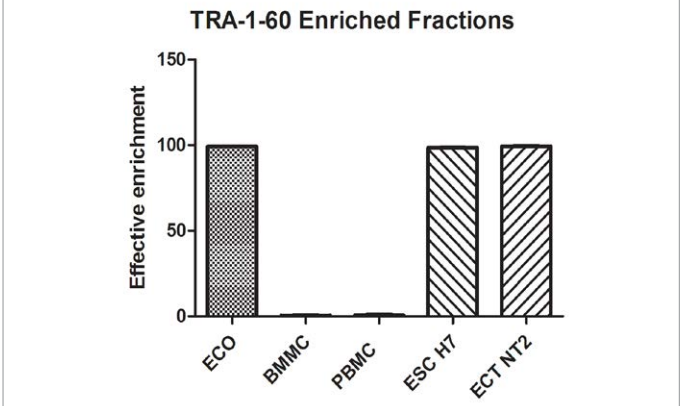

Figure 4: Purity of the enriched TRA-1-60+ ECO cells. The samples were enriched by negative selection with the superparamagnetic Fv targeting CD45, CD34, CD14, CD19, dsDNA, phosphatidylserine. That was followed by positive selection with the superparamagnetic Fv targeting TRA-1-60. This resulted in the sorts' purities > 99% with the statistical significance $p < 0.001$. Labels: ECO – patients' samples (n=6); PBMC – peripheral blood mononuclear cells (n=6); BMMC – bone marrow mononuclear cells (n=6); ESC – cultures of the human embryonic stem cells H1, H7, H9 (n=3); ECT -cultures of the human testicular embryonal carcinoma cells NT2D1 (n=1).

was performed by quantification of the labels on the blots as presented in the figure 6. The intensity of the surface display is similar to that of the ECT and ESC cells included as the positive controls. The PBMC and BMMC cells' labeling was not detected.

The analysis of the ECO display molecular profiles was also performed by immunoblotting with the Fv targeting SSEA-4 as illustrated in the figure 7. The labeling of the ECO cells is again very strong and specific. There is no label in the background. The labeling pattern is identical to that of the ESC and ECT cells. The PBMC and BMMC lanes had no labels on them. The statistical analysis is presented in the figure 8. The statistical significance was approved at the $p < 0.001$. It confirms the data from immunoblots that the display of the SSEA-4 on the ECO cells is identical to that on the ESC and ECT cells. Having the specific Fv validated in classical procedures, these Fvs were further used for initial and follow up screening for the presence of the TRA-1-60 and SSEA-4 positive cells performed with the NMR and TRXF. Measurements of the concentrations of the cell surface receptors were pursued using nuclear magnetic resonance (NMR). That was possible through measurements of the relaxation times T1 induced by labeling of the human, ovarian embryonal carcinomas with the superparamagnetic Fv (s*Fv). The labeled cultured human embryonic stem cells hESC H1, H7, H9, and testicular EC cells NT2D1 were

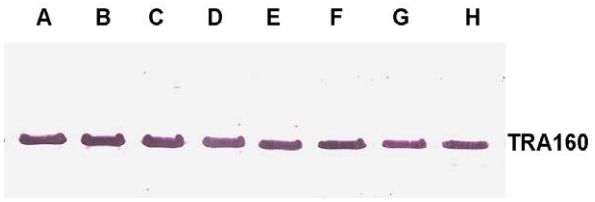

Figure 5: TRA-1-60+ display on the ECO cells. The ECO cells were disintegrated, electrophoresed, transferred onto the PVDF membranes, and labeled with the Fvs targeting TRA-1-60. Labels: ECO – patients' samples (encoded A-F); ESC – culture of the human embryonic stem cells H7 (G); ECT -culture of the human testicular embryonal carcinoma cells NT2D1 (H); PBMC – peripheral blood mononuclear cells; BMMC – bone marrow mononuclear cells (empty lanes not shown). The samples were run and quantified in triplicates. All the immunoblots were quantified as presented in the figure 6.

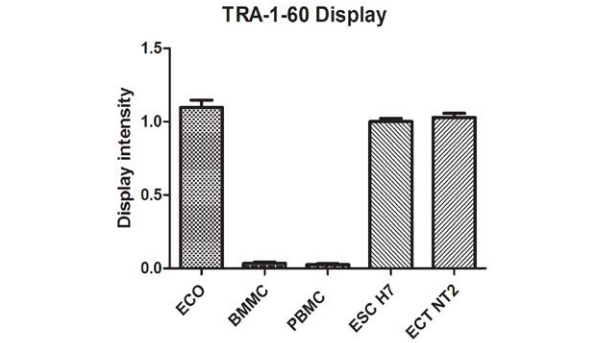

Figure 6: Quantified ECO cell surface display of TRA-1-60. The pixel intensity values were measured on the TRA-1-60 scFv labeled immunoblots of the cell lysates as described in the figure 5. Labels: ECO – patients' samples (n=6); PBMC – peripheral blood mononuclear cells (n=6); BMMC – bone marrow mononuclear cells (n=6); ESC – cultures of the human embryonic stem cells H1, H7, H9 (n=3); ECT -cultures of the human testicular embryonal carcinoma cells NT2D1 (n=1). Statistical significance accepted at the $p < 0.001$. The samples were run and quantified in triplicates.

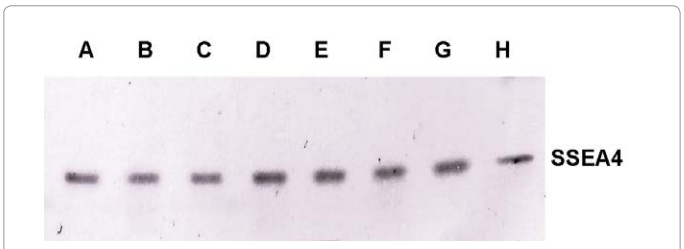

Figure 7: SSEA-4+ display on the ECO cells. The ECO cells were disintegrated, electrophoresed, transferred onto the PVDF membranes, and labeled with the Fvs targeting SSEA-4. Labels: ECO – patients' samples (encoded A-F); ESC – culture of the human embryonic stem cells H7 (G); ECT -culture of the human testicular embryonal carcinoma cells NT2D1 (H); PBMC – peripheral blood mononuclear cells; BMMC – bone marrow mononuclear cells (empty lanes not shown). The samples were run and quantified in triplicates. All the immunoblots were quantified as presented in the figure 8.

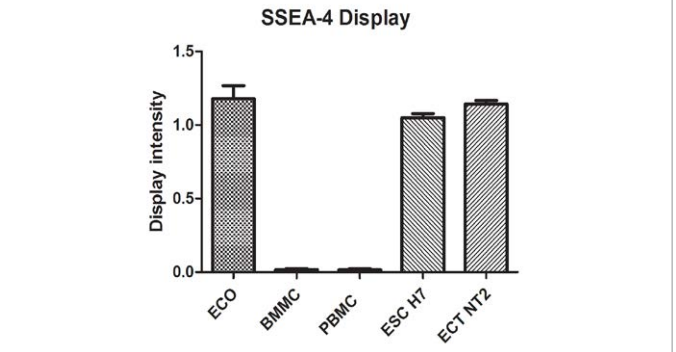

Figure 8: Quantified ECO cell surface display of SSEA-4. The pixel intensity values were measured on the SSEA-4 scFv labeled immunoblots of the cell lysates as described in the figure 7. Labels: ECO – patients' samples (n=6); PBMC – peripheral blood mononuclear cells (n=6); BMMC – bone marrow mononuclear cells (n=6); ESC – cultures of the human embryonic stem cells H1, H7, H9 (n=3); ECT -cultures of the human testicular embryonal carcinoma cells NT2D1 (n=1). Statistical significance accepted at the $p < 0.001$. The samples were run and quantified in triplicates.

again the positive controls. The PBMC and BMMC cells were negative controls. On average, T1s were falling down to ms, i.e., two orders of magnitude lower, than the relaxation times of unlabeled cells or cells' depleted sera. These data were further validated by measurements of the receptors' density by EDXS or TRXFS. The concentrations of Gd, Tb, or Eu were indicative of the number of chelated Fvs, thus the number of receptors per cell. This way of measuring the cell receptors was far less cell traumatic, faster, simpler, more sensitive alternative than running the measurements by FCM or RIA. The sensitivity of these methods was similar to those of autoradiography and scintillation, but far safer in the laboratory practice.

Transcripts of OCT4A – the main transcription factor controlling pluripotency, were studied by extraction and quantification of the total RNA followed by quantitative reverse transcription and polymerase reaction (q RT PCR). Specificity of the amplification was determined on agarose gels as illustrated in the figure 9. It shows the clean bands of the OCT4A transcripts, after being reverse transcribed and amplified. The lanes carrying amplicons for the ECO cells are identical to those for the hESC and hECT cells' cDNA used as the positive controls. The lanes hosting amplicons for the BMMC and PBMC were empty. This approach helped to eliminate a risk of including for sequencing the products of mispriming and mutations. The gels were scanned and digitized, which was followed by quantitative analysis. Quantification

of the gene expression was also accomplished with the q RT PCR as shown in the figure 10. Quantities of the OCT4A transcripts were normalized against the beta actin and GAPDH transcripts. Thereafter, the transcripts' levels were compared between the patients' versus hESC and hECT, or versus BMMC and PBMC. These measurements revealed the statistically similar levels of transcripts in the ECO cells relative to the hECT and hESC cells. The amplifications in the PBMCs and BMMCs were below the thresholds. The data were approved with the meaningful statistical significance at $p < 0.001$. Products of the OCT4A translation were determined on the cells labeled with the Fvs as illustrated in the figure 11. The OCT4A transcription factors localized into the nuclei within the ECO cells on the identical way as in the ESC and ECT cells. Transcripts of NANOG were analyzed the same way. After reverse transcription and amplification, the amplicons were electrophoresed and imaged as shown in the figure 12. The amplicons from the ECO samples were identical to those from the ECT and ESC. The PCR of the PBMC and BMMC did not result in detectable products. The levels of transcripts were also quantified by the q RT PCR relative to the GAPDH or actin, while being compared to the ESC cells as a reference. The figure 13 demonstrates that the ECO cells expressed nearly identical levels of the transcripts as the ESC and ECT. These

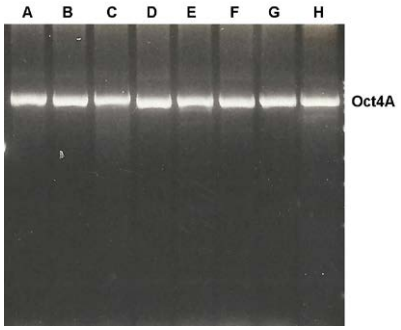

Figure 9: OCT4A gene expression in the ECO cells. The RNA from the ECO cells was reverse transcribed into cDNA, which was then amplified by polymerase chain reaction with the primers for OCT4A. Labels: ECO – patients' samples (encoded A-F); ESC – culture of the human embryonic stem cells H7 (G); ECT -culture of the human testicular embryonal carcinoma cells NT2D1 (H); PBMC – peripheral blood mononuclear cells; BMMC – bone marrow mononuclear cells (no amplicons - empty lanes not shown). Intentionally the entire lanes are shown to demonstrate specificity of amplification with the entire absence of mispriming. All the gels of amplicons were normalized and calculated with the statistical significance at the $P < 0.001$. The samples are representative for all amplifications. The samples were run in triplicates.

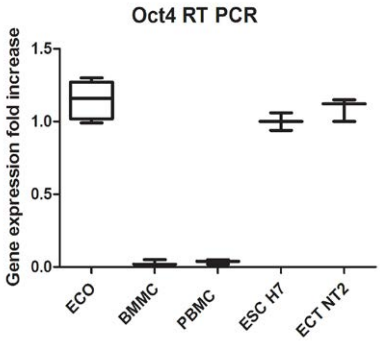

Figure 10: Quantitative analysis of the OCT4A expression in the ECO cells. The RNA from the cells was reverse transcribed into cDNA, which was then amplified by RT qPCR with the primers for the OCT4A. The amplification was calculated in relation to GAPDH and compared relative to the ESC expression. Labels: ECO – patients' samples (n=6); PBMC – peripheral blood mononuclear cells (n=6); BMMC – bone marrow mononuclear cells (n=6); ESC – cultures of the human embryonic stem cells H1, H7, H9 (n=3); ECT -cultures of the human testicular embryonal carcinoma cells NT2D1 (n=1). Statistical significance was accepted at the $p < 0.001$. The samples were run in triplicates.

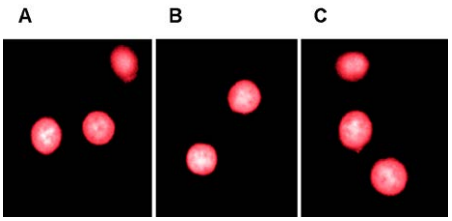

Figure 11: OCT4A gene expression products in the nuclei of the ECO cells. The cells were cryoimmobilized and labeled with the antibodies targeting OCT4A. The cells were imaged by multiphoton fluorescence microscopy. The OCT4A transcription factors are restricted to the cell nuclei. Labels: ECO – patient's sample (encoded A); ESC – culture of the human embryonic stem cells H7 (B); ECT -culture of the human testicular embryonal carcinoma cells NT2D1 (C); PBMC – peripheral blood mononuclear cells; BMMC – bone marrow mononuclear cells (no labeling – empty screens not shown).

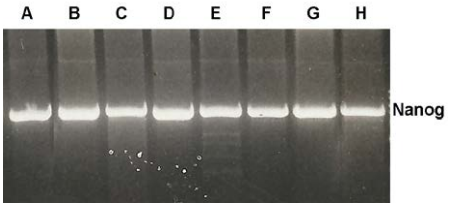

Figure 12: NANOG gene expression in the ECO cells. The RNA from the ECO cells was reverse transcribed into cDNA, which was then amplified by polymerase chain reaction with the primers for NANOG. Labels: ECO – patients' samples (encoded A-F); ESC – culture of the human embryonic stem cells H7 (G); ECT -culture of the human testicular embryonal carcinoma cells NT2D1 (H); PBMC – peripheral blood mononuclear cells; BMMC – bone marrow mononuclear cells (no amplicons - empty lanes not shown). Intentionally, the entire lanes are shown to demonstrate specificity of amplification with the entire absence of mispriming. All the gels of amplicons were normalized and calculated with the statistical significance at the $P < 0.001$. The samples were run in triplicates. The samples are representative for all amplifications.

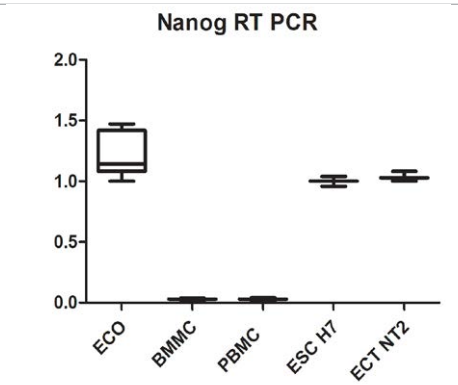

Figure 13: Quantitative analysis of the NANOG expression in the ECO cells. The RNA from the cells was reverse transcribed into cDNA, which was then amplified by RT PCR with the primers for NANOG. The amplification was calculated in relation to GAPDH and compared to the ESC expression. Labels: ECO – embryonal carcinoma of the ovary; BMMC – bone marrow mononuclear cells; PBMC – peripheral blood mononuclear cells; ESC – human embryonic stem cells; ECT – human embryonal carcinoma of the testis. The samples were run in triplicates. The data were accepted with the statistical significance $p < 0.001$.

transcripts were not detected in the PBMC and BMMC. The data were accepted with the statistical significance the value $p < 0.001$.

Functional tests of the ECO cells' pluripotency involved culturing embryoid bodies and checking their ability to differentiate into the three germ layers as summarized in the figure 14. Within days, the biomarkers of differentiation were clearly detected. Antibodies to the NF68 neurofilaments, cardiac muscle myosin, and CK18 cytokeratins reported differentiation towards ectoderm, mesoderm, and endoderm respectively. The pluripotency of the ECO cells was further confirmed upon inducing their differentiation after plating them into the matrigel matrix. The cells were homogenized, electrophoresed, and transferred onto the PVDF membranes. The samples on the membranes were labeled with the Fvs and imaged as illustrated in the figures 15-17. The DMSO and HMBA induction of the ECO cells differentiation into the muscle was demonstrated by presence of very strong and specific bands of the cardiac muscle myosin shown in the figure 15. The specificity was validated by blots of the human cardiac muscle and the ESC induced to differentiate on the same way, which were used as the positive controls being. The EGF induced the ECO cells to differentiate into the epithelia as presented in the figure 16. The specificity of labeling was validated by the positive controls of the ESC also induced to differentiate and the healthy ovarian tissue. The RA and NGF induced differentiation into neurons. This resulted in the expression of the NF68 neurofilaments

Epitope	Marker	Embryoid bodies						
		A	B	C	D	E	F	G
Neurofilament 68kDa	Ectoderm	+++	+-+	+++	+++	+++	+-+	+++
Muscle myosin	Mesoderm	+++	++L	++-	+++	+++	+++	+++
Cytokeratin	Endoderm	++L	+++	++-	+++	+++	+++	+++

Figure 14: Formation of embryoid bodies and differentiation into three main germ layers. The embryoid bodies were tested by labeling with the antibodies targeting neurofilaments protein (68kDa) as the biomarker for the forming ectoderm; muscle myosin for the mesoderm; and cytokeratins for the endoderm. Labels: the embryoid bodies from the ECO cells (A-F), embryonic stem cells (H7) (G); (negative controls not included); +: positive reaction; -: negative reaction; L: lost sample.

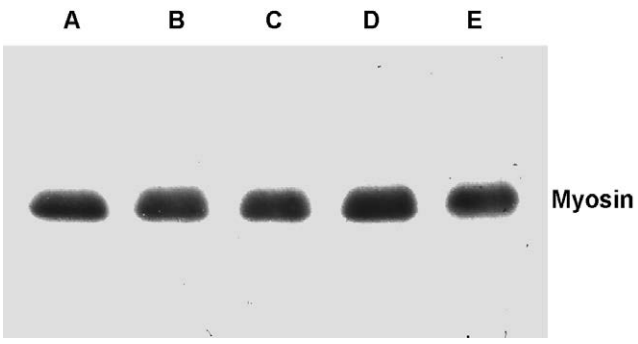

Figure 15: Differentiation of the ECO cells into muscle. The ECO cells were induced to differentiate into the cardiac muscles. The cells were homogenized, electrophoresed, and transferred onto the PVDF membranes. The transfers on the membranes were labeled with the antibodies against cardiac muscle myosin. Labels: ECO – patients' samples (encoded A-C); cardiac muscle myosin (D); human cardiac muscle (E); PBMC – peripheral blood mononuclear cells; BMMC – bone marrow mononuclear cells (no labeling - empty lanes not shown).

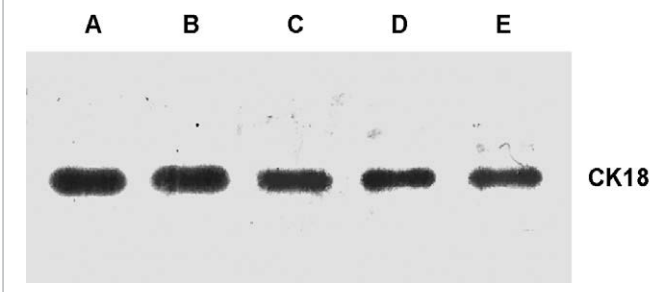

Figure 16: Differentiation of the ECO cells into epithelium. The ECO cells were induced to differentiate into the epithelium. The cells were homogenized, electrophoresed, and transferred onto the PVDF membranes. The transfers on the membranes were labeled with the antibodies against CK18 keratins. Labels: ECO – patients' samples (encoded A-C); CK18 cytokeratin (D); healthy ovary tissue (E); PBMC – peripheral blood mononuclear cells; BMMC – bone marrow mononuclear cells (no labeling - empty lanes not shown).

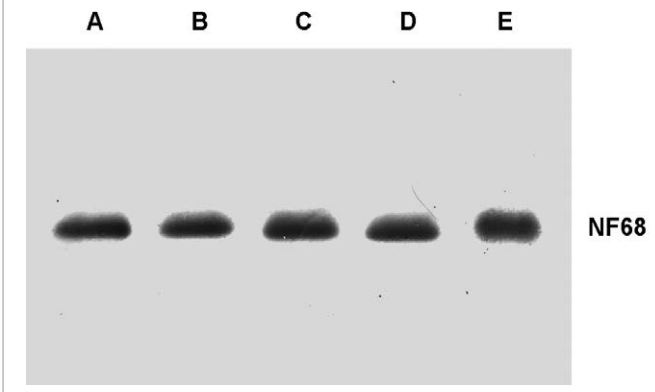

Figure 17: Differentiation of the ECO cells into neurons. The ECO cells were induced to differentiate into the neurons. The cells were homogenized, electrophoresed, and transferred onto the PVDF membranes. The transfers on the membranes were labeled with the antibodies against the NF68 neurofilaments. Labels: ECO – patients' samples (encoded A-C); NF68 neurofilaments (D); human healthy brain tissue (E); PBMC – peripheral blood mononuclear cells; BMMC – bone marrow mononuclear cells (no labeling - empty lanes not shown).

revealed as the strong band on the immunoblots in the figure 17. The brain tissue obtained from the healthy margins excised during brain surgery and human embryonic stem cells induced to differentiate facilitated the validation of the data.

Discussion

A few elements of biotechnology, which we applied here, are worth stressing. First, we used rapid cryo-immobilization to capture the living-like cells' morphology and molecules' properties. It is a common misconception that freezing in liquid nitrogen offers the fast freezing rate associated with the better preservation of viability and antigenicity. As the matter of fact, due to the Leidenfrost's effect, the boiling around the sample delays cooling significantly. Therefore, we used the approach, which provided a much faster freezing rate, thus assured instant preservation of molecules properties. Second, it is a well known fact that the chemical fixation or slow freezing may dramatically change epitopes, so that the antibodies, which were developed for the native molecules may not work with the denatured proteins. Therefore, the antibodies used for Western blotting are rarely useful for native immunoblotting. For these reasons, we preferred working with the

native or rapidly frozen specimens, which offered direct extrapolation of the data for the in vivo environment. Third, FACS on fluorescently labeled cells inflicts a severe shearing stress due to pressurized tubes guiding the cells, which results in a very low viability in addition to the poor staining. Plans for clonal expansion, inducing differentiation, and drug testing, could be jeopardized by low viability of the isolated cells. Therefore, we engineered superparamagnetic variable fragment antibody biotags (scFv) and magnetic sorter, which allowed us to gently isolate the labeled cells by means of magnetic forces, thus assuring high viability. Fourth, the small size of our Fvs helped in overcoming steric hindrance forces and assuring high density packing onto the receptors. Their high specificity and sensitivity resulted in heavy labeling of the receptors and practical absence of non-specific labeling of other cells, which translated in the high signal to noise ratios.

Using these technologies, we revealed the populations of the pluripotent, cancer stem cells in the embryonal carcinomas of the ovaries. Moreover, we demonstrated that the levels of gene expression for the Nanog and OCT4A transcription factors were equivalent or higher in the ECO cells, than they were in the cultured embryonic stem cells and testicular embryonal carcinoma cells. Importantly, they were statistically significantly different compared to healthy control cells. These differences were detected with the highly sensitive means of detection possible after cycles of amplification in PCR. Therefore, they could be applied on the standard FFPE sections after selection, deparafanization, and amplification or alternatively on cryo-sections. The mononuclear cells from the same patients were showing no expression, while serving as the additional controls for these diagnostic tests.

Moreover, these data contribute to raising hypotheses on initiating neoplasms. First, neoplasms of the ovaries may develop *de novo* from one or a few pluripotent stem cells present in the ovaries. With the tumor progression, some of the cells partially differentiate, which helps in determination of their lineages. As it happens, they may be used for immuno-histopathological classification. Nevertheless, the stem cells are at the core of these processes as carcinoma *in situ*. Second, progression of the neoplasms leads to progressive accumulation of the mutations, which may turn on the transcription factors of pluripotency and cause generation of the clones of stem cells. Third, therapies effectively regulate the selection process to eliminate sensitive clones, while leaving room for the therapy resistant cancer cells. Therefore, they should be the targets of specifically designed therapies. Nevertheless, the cancer stem cells have to compete for spaces and nutrients with other cancer cells. Only after elimination of therapy sensitive cells, the cancer stem cells lose their competition and drive progression of the disease. These processes of selection may occur at the consecutive stages of the tumor progression and consecutive regimes of therapy. Initially, some clones breaking away from the primary tumors may find suitable environment for advancing along the FIGO clinical stages I to II. Among them or from them, raise the clones capable to attach to endothelium or peritoneum, what leads to the progression of the disease to the FIGO stages III and IV. In all these scenarios, capturing and detailed molecular profiling of the cells, which break away from the ECO is essential for intercepting these cells, thus blocking progression of cancer.

The current approach in administering the therapies to the patients is based upon trials and errors, while watching for the responses and adjusting the therapeutic regimes *ex iuvantibus*. The novel approaches towards cancer molecular profiling should help us to craft the patient individualized therapy and pursue effective biomarker-targeted, patient-centered personalized therapy.

Conclusion

Herein, we revealed presence and identify molecular profiles of the clones of the pluripotent stem cells in the embryonal carcinomas of the ovaries. These results should help us with refining molecular diagnoses of these deadly neoplasms.

Acknowledgment

First of all, we thank the patients for their consent. We thank Dr. J. Pietruszkiewicz, Dr. L. Sikorowa, and Dr. J. Szymendera for providing some of the samples. We thank for providing primers, hexamers, monoclonal antibodies, and embryonic stem cells by Dr. J. Antosiewicz, Dr M. L. Greaser, Dr T. Kunicki, Dr J.V. Small, Dr. J. Swiergiel, Dr. W. Szybalski, and Dr. J. Thomson. We acknowledge with thanks access to the NIH National Nuclear Magnetic Resonance Facility, the SDSU Functional Genomics Center, Bruker AXS Laboratories, Bruker Optics Laboratories, and the NIH IMR National Biotechnology Resource. We also thank Dr S. Jeffrey, Dr. J. Langmore, Dr. E. Lianidou, Dr J. Markley, Dr. M. Marchetti, Dr. P. Paterlini, Dr. E. Rajpert-DeMeyts, and Dr W. Szybalski for the discussions.

This work was supported by the funds from the NIH, NCRR, GM103399, RR000570, from the NSF 9420056, 9522771, 9902020, and 0094016, and from the PBMEF. The work was pursued at the National Biotechnology Resource, NIH, the Molecular Imaging Laboratory, UCSD, the National Biomedical NMR Resource, NIH, McArdle Cancer Research Laboratories, UW, the PBMEF, the BioSpin, the Bruker Optics, and the Genomics Center, SDSU; therefore the access to the instrumentation at those laboratories is gratefully acknowledged.

References

1. Jemal A, Siegel R, Xu J, Ward E (2010) Cancer statistics, 2010. CA Cancer J Clin 60: 277-300.
2. Kosary CL (2007) Cancer of the Ovary. In: Ries LAG et al., editors. SEER survival monograph: Cancer survival among adults : US SEER program, 1988-2001, patient and tumor characteristics. Bethesda, MD: U.S. Department of Health and Human Services, National Institutes of Health, National Cancer Institute: 1-12.
3. Pecorelli S, Benedet JL, Creasman WT, Shepherd JH (1999) FIGO staging of gynecologic cancer. 1994-1997 FIGO Committee on Gynecologic Oncology. Int J Gynaecol Obstet 65: 243-249.
4. Bankhead CR, Kehoe ST, Austoker J (2009) Symptoms associated with diagnosis of ovarian cancer: a systematic review. BJOG 112: 857-865.
5. Ryerson AB, Eheman C, Burton J, McCall N, Blackman D, et al. (2007) Symptoms, diagnoses, and time to key diagnostic procedures among older U.S. women with ovarian cancer. Obstet Gynecol 109: 1053-1061.
6. Goff BA, Mandel LS, Melancon CH, Muntz HG (2004) Frequency of symptoms of ovarian cancer in women presenting to primary care clinics. JAMA 291: 2705-2712.
7. Memarzadeh S, Lee SB, Berek JS, Farias-Eisner R (2003) CA125 levels are a weak predictor of optimal cytoreductive surgery in patients with advanced epithelial ovarian cancer. Int J Gynecol Cancer 13: 120-124.
8. Lianidou ES, Markou A (2011) Circulating tumor cells as emerging tumor biomarkers in breast cancer. Clin Chem Lab Med 49: 1579-1590.
9. Paterlini-Bréchot P (2011) Organ-specific markers in circulating tumor cell screening: an early indicator of metastasis-capable malignancy. Future Oncol 7: 849-871.

10. Nosov V, Su F, Amneus M, Birrer M, Robins T, et al. (2009) Validation of serum biomarkers for detection of early-stage ovarian cancer. Am J Obstet Gynecol 200: 639.e1-5.

11. Karam AK, Karlan BY (2010) Ovarian cancer: the duplicity of CA125 measurement. Nat Rev Clin Oncol 7: 335-339.

12. Yurkovetsky Z, Skates S, Lomakin A, Nolen B, Pulsipher T, et al. (2010) Development of a multimarker assay for early detection of ovarian cancer. J Clin Oncol 28: 2159-2166.

13. Hennessy BT, Murph M, Nanjundan M, Carey M, Auersperg N, et al. (2008) Ovarian cancer: linking genomics to new target discovery and molecular markers--the way ahead. Adv Exp Med Biol 617: 23-40.

14. Marrink J, Andrews PW, van Brummen PJ, de Jong HJ, Sleijfer DT, et al. (1991) TRA-1-60: a new serum marker in patients with germ-cell tumors. Int J Cancer 49: 368-372.

15. Helleman J, Jansen MP, Burger C, van der Burg ME, Berns EM (2010) Integrated genomics of chemotherapy resistant ovarian cancer: a role for extracellular matrix, TGFbeta and regulating microRNAs. Int J Biochem Cell Biol 42: 25-30.

16. Mezzanzanica D, Bagnoli M, De Cecco L, Valeri B, Canevari S (2010) Role of microRNAs in ovarian cancer pathogenesis and potential clinical implications. Int J Biochem Cell Biol 42: 1262-1272.

17. van Jaarsveld MT, Helleman J, Berns EM, Wiemer EA (2010) MicroRNAs in ovarian cancer biology and therapy resistance. Int J Biochem Cell Biol 42: 1282-1290.

18. Giordano A, Giuliano M, De Laurentiis M, Arpino G, Jackson S, et al. (2011) Circulating tumor cells in immunohistochemical subtypes of metastatic breast cancer: lack of prediction in HER2-positive disease treated with targeted therapy. Ann Oncol 23: 1144-1150.

19. Rao A, Carter J (2011) Ultrasound and ovarian cancer screening: is there a future? J Minim Invasive Gynecol 18: 24-30.

20. Menon U, Gentry-Maharaj A, Hallett R, Ryan A, Burnell M, et al. (2009) Sensitivity and specificity of multimodal and ultrasound screening for ovarian cancer, and stage distribution of detected cancers: results of the prevalence screen of the UK Collaborative Trial of Ovarian Cancer Screening (UKCTOCS). Lancet Oncol 10: 327-340.

21. Shin DS, Poder L, Courtier J, Naeger DM, Westphalen AC, et al. (2011) CT and MRI of early intrauterine pregnancy. AJR Am J Roentgenol 196: 325-330.

22. Kurman RJ, Norris HJ (1976) Embryonal carcinoma of the ovary: a clinicopathologic entity distinct from endodermal sinus tumor resembling embryonal carcinoma of the adult testis. Cancer 38: 2420-2433.

23. Chobanian N, Dietrich CS 3rd (2008) Ovarian cancer. Surg Clin North Am 88: 285-299.

24. Dean M, Fojo T, Bates S (2005) Tumour stem cells and drug resistance. Nat Rev Cancer 5: 275-284.

25. Diehn M, Cho RW, Lobo NA, Kalisky T, Dorie MJ, et al. (2009) Association of reactive oxygen species levels and radioresistance in cancer stem cells. Nature 458: 780-783.

26. Sokolov MV, Panyutin IV, Onyshchenko MI, Panyutin IG, Neumann RD (2010) Expression of pluripotency-associated genes in the surviving fraction of cultured human embryonic stem cells is not significantly affected by ionizing radiation. Gene. 455: 8-15.

27. Milas L, Hittelman WN (2009) Cancer stem cells and tumor response to therapy: current problems and future prospects. Semin Radiat Oncol 19: 96-105.

28. Nicolini A, Ferrari P, Fini M, Borsari V, Fallahi P, et al. (2011) Stem cells: their role in breast cancer development and resistance to treatment. Curr Pharm Biotechnol 12: 196-205.

29. Malecki M, Szybalski W (2012) Isolation of single, intact chromosomes from single, selected ovarian cancer cells for in situ hybridization and sequencing. Gene 493: 132-139.

30. Navin N, Hicks J (2011) Future medical applications of single-cell sequencing in cancer. Genome Med 3: 31.

31. Zhang J, Guo X, Chang DY, Rosen DG, Mercado-Uribe I, et al. (2011) CD133 expression associated with poor prognosis in ovarian cancer. Mod Pathol 25: 456-464.

32. Alvero AB, Montagna MK, Holmberg JC, Craveiro V, Brown D, et al. (2012) Targeting the mitochondria activates two independent cell death pathways in ovarian cancer stem cells. Mol Cancer Ther 10: 1385-1393.

33. Fong MY, Kakar SS (2010) The role of cancer stem cells and the side population in epithelial ovarian cancer. Histol Histopathol 25: 113-120.

34. Kryczek I, Liu S, Roh M, Vatan L, Szeliga W, et al. (2012) Expression of aldehyde dehydrogenase and CD133 defines ovarian cancer stem cells. Int J Cancer 130: 29-39.

35. Sillanpää S, Anttila MA, Voutilainen K, Tammi RH, Tammi MI, et al. (2003) CD44 expression indicates favorable prognosis in epithelial ovarian cancer. Clin Cancer Res 9: 5318-5324.

36. Guo R, Wu Q, Liu F, Wang Y (2011) Description of the CD133+ subpopulation of the human ovarian cancer cell line OVCAR3. Oncol Rep 25: 141-146.

37. Rodríguez-Rodríguez L, Sancho-Torres I, Mesonero C, Gibbon DG, Shih WJ, et al. (2003) The CD44 receptor is a molecular predictor of survival in ovarian cancer. Med Oncol 20: 255-263.

38. Naor D, Wallach-Dayan SB, Zahalka MA, Sionov RV (2008) Involvement of CD44, a molecule with a thousand faces, in cancer dissemination. Semin Cancer Biol 18: 260-267.

39. Nam EJ, Lee M, Yim GW, Kim JH, Kim S, et al. (2012) MicroRNA profiling of a CD133+ spheroid-forming subpopulation of the OVCAR3 human ovarian cancer cell line. BMC Med Genomics 5: 18.

40. Friedrichs K, Franke F, Lisboa BW, Kügler G, Gille I, et al. (1995) CD44 isoforms correlate with cellular differentiation but not with prognosis in human breast cancer. Cancer Res 55: 5424-5433.

41. Zhu Y, Huang JM, Zhang GN, Zha X, Deng BF (2012) Prognostic significance of MyD88 expression by human epithelial ovarian carcinoma cells. Molecular phenotyping of human ovarian cancer stem cells unravels the mechanisms for repair and chemoresistance. J Transl Med 10: 77.

42. Kim KH, Jo MS, Suh DS, Yoon MS, Shin DH, et al. (2012) Expression and significance of the TLR4/MyD88 signaling pathway in ovarian epithelial cancers. World J Surg Oncol 10: 193.

43. Andrews PW, Damjanov I, Simon D, Banting GS, Carlin C, et al. (1984) Pluripotent embryonal carcinoma clones derived from the human teratocarcinoma cell line Tera-2. Lab Invest 50: 147-162.

44. Damjanov I, Andrews PW (1983) Ultrastructural differentiation of a clonal human embryonal carcinoma cell line in vitro. Cancer Res 43: 2190-2198.

45. Andrews PW, Banting G, Damjanov I, Arnaud D, Avner P (1984) Three monoclonal antibodies defining distinct differentiation antigens associated with different high molecular weight polypeptides on the surface of human embryonal carcinoma cells. Hybridoma 3: 347-361.

46. Andrews PW, Matin MM, Bahrami AR, Damjanov I, Gokhale P, et al. (2005) Embryonic stem (ES) cells and embryonal carcinoma (EC) cells: opposite sides of the same coin. Biochem Soc Trans 33: 1526-1530.

47. Sperger JM, Chen X, Draper JS, Antosiewicz JE, Chon CH, et al. (2003) Gene expression patterns in human embryonic stem cells and human pluripotent germ cell tumors. Proc Natl Acad Sci USA 100: 13350-13355.

48. Malecki M, Pietruszkiewicz J, Ratajczak M (2006) Nanoengineered antibodies against embryonal carcinoma's SSEA-3, SSEA-4, TRA-1-60, and TRA-1-81 demonstrate presence of pluripotent cells in situ, in healthy human bone marrow. European Journal of Surgical Oncology 32: 1.

49. Chaerkady R, Kerr CL, Kandasamy K, Marimuthu A, Gearhart JD, et al. (2010) Comparative proteomics of human embryonic stem cells and embryonal carcinoma cells. Proteomics 10: 1359-1373.

50. Pashai N, Hao H, All A, Gupta S, Chaerkady R, et al. (2012) Genome-wide profiling of pluripotent cells reveals a unique molecular signature of human embryonic germ cells. PLoS One 7: e39088.

51. Andrews PW (1984) Retinoic acid induces neuronal differentiation of a cloned human embryonal carcinoma cell line in vitro. Dev Biol 103: 298-293.

52. Tonge PD, Andrews PW (2010) Retinoic acid directs neuronal differentiation

of human pluripotent stem cell lines in a non-cell-autonomous manner. Differentiation 80: 20-30.

53. Rao RR, Johnson AV, Stice SL (2007) Cell surface markers in human embryonic stem cells. Methods Mol Biol 407: 51-61.

54. Biermann K, Heukamp LC, Steger K, Zhou H, Franke FE, et al. (2007) Gene expression profiling identifies new biological markers of neoplastic germ cells. Anticancer Res 27: 3091-3100.

55. Almstrup K, Hoei-Hansen CE, Wirkner U, Blake J, Schwager C, et al. (2004) Embryonic stem cell-like features of testicular carcinoma in situ revealed by genome-wide gene expression profiling. Cancer Res 64: 4736-4743.

56. Giwercman A, Andrews PW, Jørgensen N, Müller J, Graem N, et al. (1993) Immunohistochemical expression of embryonal marker TRA-1-60 in carcinoma in situ and germ cell tumors of the testis. Cancer 72: 1308-1314.

57. Gels ME, Marrink J, Visser P, Sleijfer DT, Droste JH, et al. (1997) Importance of a new tumor marker TRA-1-60 in the follow-up of patients with clinical stage I nonseminomatous testicular germ cell tumors. Ann Surg Oncol 4: 321-327.

58. Pera MF, Bennett W, Cerretti DP (1997) Expression of CD30 and CD30 ligand in cultured cell lines from human germ-cell tumors. Lab Invest 76: 497-504.

59. Cheng L, Sung MT, Cossu-Rocca P, Jones TD, MacLennan GT, et al. (2007) OCT4: biological functions and clinical applications as a marker of germ cell neoplasia. J Pathol 211: 1-9.

60. Jones TD, MacLennan GT, Bonnin JM, Varsegi MF, Blair JE, et al. (2006) Screening for intratubular germ cell neoplasia of the testis using OCT4 immunohistochemistry. Am J Surg Pathol 30: 1427-1431.

61. Hoei-Hansen CE, Kraggerud SM, Abeler VM, Kaern J, Rajpert-De Meyts E, et al. (2007) Ovarian dysgerminomas are characterised by frequent KIT mutations and abundant expression of pluripotency markers. Mol Cancer 6: 12.

62. Hart AH, Hartley L, Parker K, Ibrahim M, Looijenga LH, et al. (2005) The pluripotency homeobox gene NANOG is expressed in human germ cell tumors. Cancer 104: 2092-2098.

63. Fogh J (1978) Cultivation, characterization, and identification of human tumor cells with emphasis on kidney, testis, and bladder tumors. Nati Cancer Inst Monogr 49: 5-9.

64. Mueller-Klieser W (1997) Three-dimensional cell cultures: from molecular mechanisms to clinical applications. Am J Physiol 273: C1109-C1123.

65. Sidhu KS, Tuch BE (2006) Derivation of three clones from human embryonic stem cell lines by FACS sorting and their characterization. Stem Cells Dev 15: 61-69.

66. Talasaz AH, Powell AA, Huber DE, Berbee JG, Roh KH, et al. (2009) Isolating highly enriched populations of circulating epithelial cells and other rare cells from blood using a magnetic sweeper device. Proc Natl Acad Sci USA 106: 3970-3975.

67. Malecki M, Hsu A, Truong L, Sanchez S (2002) Molecular immunolabeling with recombinant single-chain variable fragment (scFv) antibodies designed with metal-binding domains. Proc Natl Acad Sci USA 99: 213-218.

68. Malecki M, Malecki R (2012) Multidomain biotags for cancer detection, diagnosis, and therapy, and methods of their use. USPTO US20120093733: 1-187.

69. Fong CY, Peh GS, Gauthaman K, Bongso A (2009) Separation of SSEA-4 and TRA-1-60 labelled undifferentiated human embryonic stem cells from a heterogeneous cell population using magnetic-activated cell sorting (MACS) and fluorescence-activated cell sorting (FACS). Stem Cell Rev 5: 72-80.

70. Malecki M, Malecki B (2011) Methods for Manufacturing and Using of Molecular Death Tags. WIPO. WO2011162904: 1-123.